Citation: Basereh, S., Okumus, P., Aaleti, S. (2020) "Reinforced Concrete Shear Walls Retrofitted Using Weakening and Self-Centering: Numerical Modeling." ASCE Journal of Structural Engineering, 146(7), https://doi.org/10.1061/(ASCE)ST.1943-541X.0002669

Reinforced Concrete Shear Walls Retrofitted Using Weakening and Self-Centering: Numerical Modeling

Sina Basereh[1], Pinar Okumus[2], Sriram Aaleti[3]

Abstract

This paper investigates a novel retrofit strategy for code-deficient reinforced concrete (RC) shear walls that are vulnerable to undesirable failure modes. The strategy combines weakening by partially cutting the wall base and self-centering by adding post-tensioning. RC walls in need of retrofit were analyzed under lateral cyclic loading using 3-D finite element modeling. Analyses were validated using test data from the literature on conventional walls that failed in flexure/shear and pure shear. These analyses were used to study the retrofit strategy. A parametric study was conducted to determine the working details of the retrofit method. A method was proposed to select retrofit parameters preliminarily. Retrofitted and original walls were compared. The sequence in which wall components failed was documented to identify changes in failure modes. Results of the analyses showed that although retrofitting reduced energy dissipation capacity, flexural displacements increased due to retrofit of poorly designed RC walls suffering from partial or pure shear failure. Retrofit resulted in fewer cracks, less intense concrete crushing, and a delayed fracture of transverse reinforcement.

Author Keywords: Slender RC wall; Code-deficient; Cyclic loading; Numerical modeling; Retrofit; Weakening; Seismic; Post-tension; Shear failure.

[1] Graduate Research Assistant, Dept. of Civil, Structural, and Environmental Engineering, University at Buffalo, Buffalo, NY 14260 (corresponding author). Email: sinabase@buffalo.edu
[2] Associate Professor, Dept. of Civil, Structural, and Environmental Engineering, University at Buffalo, Buffalo, NY 14260. Email: pinaroku@buffalo.edu
[3] Associate Professor, Dept. of Civil, Construction and Environmental Engineering, the University of Alabama, Tuscaloosa, AL 35487. Email: saaleti@eng.ua.edu

Introduction

Many RC buildings designed prior to ACI 318-71 (ACI 1971) have slender (height-to-length ratio ≥ 2) shear walls that do not meet the requirements of the modern seismic codes (e.g., lack of well-confined boundary elements). These walls may experience shear dominated failure modes: diagonal tension due to the fracture of transverse reinforcement, diagonal compression prior to the yielding of shear reinforcement, or sliding shear (FEMA 1998; Kam and Pampanin 2011; Wallace 2012). Such shear walls require seismic retrofit. ASCE 41-17 (ASCE 2017) provides procedures to assess the seismic vulnerability of existing buildings using a three tiered approach: Tier 1 (screening phase) to Tier 3 (systematic evaluation and retrofit phase). Older buildings with shear walls can be evaluated using these procedures to determine their need for retrofit.

Traditional retrofit strategies generally strengthen walls by adding materials. A common approach is to use externally bonded steel or fiber reinforced polymer (FRP) strips or wraps. Steel strips bolted onto RC walls have been shown to increase strength, stiffness and ductility (Taghdi et al. 2000), prevent bar buckling and control web crack widths (Christidis et al. 2016). Externally bonded FRP sheets increased flexural strength and ductility when fibers are oriented vertically, and increased shear strength when fibers were aligned horizontally (Khalil and Ghobarah 2005; Lombard et al. 2000; Paterson and Mitchell 2003). Others retrofitted and repaired walls that have already been damaged (Antoniades et al. 2003; Fiorato et al. 1983; Lefas and Kotsovos 1990). Elnashai and Pinho (1998) proposed a retrofit approach by selectively intervening with stiffness, strength, ductility, one at a time, to be able to optimize the global seismic response based on the seismic demand or the previous damage state.

Traditional retrofitting methods prevent collapse but do not provide resiliency and seismic damage control, potentially leaving buildings inoperable after a major seismic event due to large residual displacements. The retrofit strategy investigated in this paper integrates self-centering and weakening. Self-centering minimizes residual displacements. Selective weakening reduces accelerations and, therefore, force demand on a system. In addition to preventing collapse, this strategy can create buildings that can be reoccupied rapidly after an earthquake by minimizing residual displacements and damage to RC shear walls. A short review of self-centering and selectively weakened structures is provided here to explain the features of the retrofit method.

Self-centering is the ability of a structure to return to its original position upon unloading, minimizing residual displacements. When rocking is the mechanism for self-centering, self-weight or unbonded post-tensioning strands can be used to create a restoring force. Self-centering with unbonded post-tensioning and sacrificial energy dissipaters have been studied for new precast concrete beam-column joints and precast walls (Holden et al. 2003; Kurama 2002; Nakaki et al. 1999; Priestley et al. 1999; Priestley and Tao 1993; Rahman and Restrepo 2000; Restrepo and Rahman 2007; Sritharan et al. 2015; Stanton et al. 1997) and for new bridge piers (Lee et al. 2007; Marriott et al. 2009; Ou et al. 2007; Palermo et al. 2007; Yang and Okumus 2017). As a retrofit method, rocking has been investigated for steel bridge piers (Pollino and Bruneau 2007).

Energy dissipation can be provided through external or internal energy dissipation mechanisms. These include O-shaped (Henry et al. 2010) or U-shaped plates for precast walls (Priestley et al. 1999), low yield strength, tapered vertical reinforcement between wall and foundation, and dog-bone shaped mild reinforcing bars (Holden et al. 2003; Rahman and Restrepo 2000; Restrepo and Rahman 2007). These systems exhibit flag-shape hysteretic behavior.

Weakening or selective weakening is a retrofit strategy in which elements of a structure are weakened (reduction of strength or stiffness) to reduce the force demand on the system. As a trade-off, displacement demand may increase (Viti et al. 2006). To accommodate the increased displacement demands, achieve target performance levels and meet capacity design principles, weakened systems may be supplemented by external reinforcement, plates or strands, damping devices, or jacketing (Kam and Pampanin 2008; Kam and Pampanin 2010; Pampanin 2006).

Ireland et al. (2007) tested selectively weakened RC walls. The retrofit technique incorporated vertical and horizontal wall cuts and the addition of post-tensioned strands. Unlike the study that is presented in this paper, Ireland et al. (2007) had the entire wall base and all reinforcement bars cut, necessitating the addition of external energy dissipaters. The retrofit resulted in higher or lower strength, and smaller residual displacements.

The literature shows that self-centering and weakening, separately, are promising concepts. This study combined these two concepts for the retrofit of code-deficient RC shear walls. Validated finite element models of code-deficient shear walls were used to understand the benefits of the retrofit method with varying parameters. Pre- and post-retrofit cyclic behaviors of walls were compared in terms of energy dissipation, lateral strength, residual displacement, secant stiffness, strain fields and failure modes.

The Retrofit Strategy

The strategy combines the concepts of selective weakening and self-centering. A RC wall is first weakened by partially cutting its base at the foundation level, together with a selected number of vertical bars. The remaining bars provide energy dissipation through yielding. To provide self-centering, unbonded post-tensioned strands are added to the wall and anchored at the foundation. A schematic of the retrofit strategy is shown in Fig. 1.

The effectiveness of the retrofit strategy is investigated through nonlinear finite element analysis (FEA) of two walls that were known to fail under shear dominated (i.e. formation of diagonal shear cracks mostly at the mid-height of the wall) or shear-flexure (core crushing) dominated failure modes. Other failure modes including bond slip failure or vertical bar buckling were out of the scope of this study.

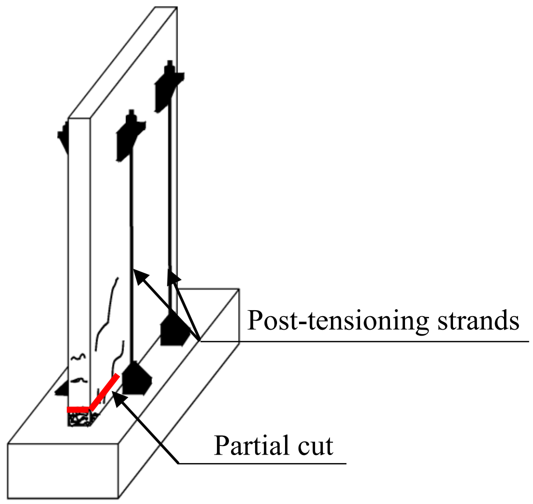

Fig. 1. Schematic sketch of retrofit strategy

Research Significance

Although concepts of weakening and self-centering on walls have been separately explored before, this study is one of the very few that combines the two strategies for resilient retrofit. Previous studies on retrofit with weakening and self-centering on walls were experimental (Ireland et al. 2007) and therefore investigated a limited number of cases or had simplified analyses under monotonic loading. The present study uses detailed analyses of walls under cyclic lateral loading to study various strategies including leaving a portion of vertical reinforcing bars uncut for energy dissipation and cutting only part of the wall base, which have never been investigated before for studies on retrofit. Existing studies (Ireland et al. 2007) used external energy dissipation methods and created full cuts at wall base for fully rocking walls. In the present study, detailed finite element models enable evaluation of fracture of bars, crushing of concrete, cracking across entire wall height.

RC Walls Used for the Analyses

Two 1:2.5 scale, slender, non-code-compliant walls (named SW6 and SW5) tested under quasi-static, lateral cyclic loading with 2 mm (0.08 in.) displacement increments to failure by Pilakoutas and Elnashai (1995) were used for the analyses. Both walls had aspect ratio of 2 and were 60 mm (2.4 in.) thick. The boundary element lengths were 110 mm (4.3 in.) and 60 mm (2.4 in.) for SW6 and SW5, respectively. Flexural and transverse reinforcement ratios of wall webs were greater than 0.25%, as required by ACI 318-14 (ACI 2014). However, walls were not compliant with ACI 318-14 in terms of boundary element requirements. For the walls under consideration, the heights of the special boundary elements were 10% (for SW6) and 13% (for SW5) shorter than the minimum height required by ACI 318-14 (ACI 2014). The vertical confining reinforcement spacing in the boundary element was 1.47 times (for SW6) and 4.40 times (for SW5) the maximum spacing required by ACI 318-14 for special structural walls.

Laboratory tests showed that walls failed partially or fully due to shear, an undesired failure mode for slender RC shear walls, making them suitable candidates for retrofit. SW6 was reported to have failed due to fracture of transverse reinforcement and crushing of concrete in the boundary element. The failure mode was concluded to be a combination of shear and concrete crushing (flexure-shear). SW5 was reported to have failed due to the fracture of transverse reinforcement and large diagonal cracks. The failure mode of SW5 was determined to be shear (Pilakoutas 1990; Pilakoutas and Elnashai 1995). The walls were tested with no axial load. Fig. 2 shows the details of RC walls selected for modeling.

Finite Element Analysis of RC Walls

RC shear walls were modeled using nonlinear FEA using a general purpose commercial FEA software, LS-DYNA (LSTC 2017).

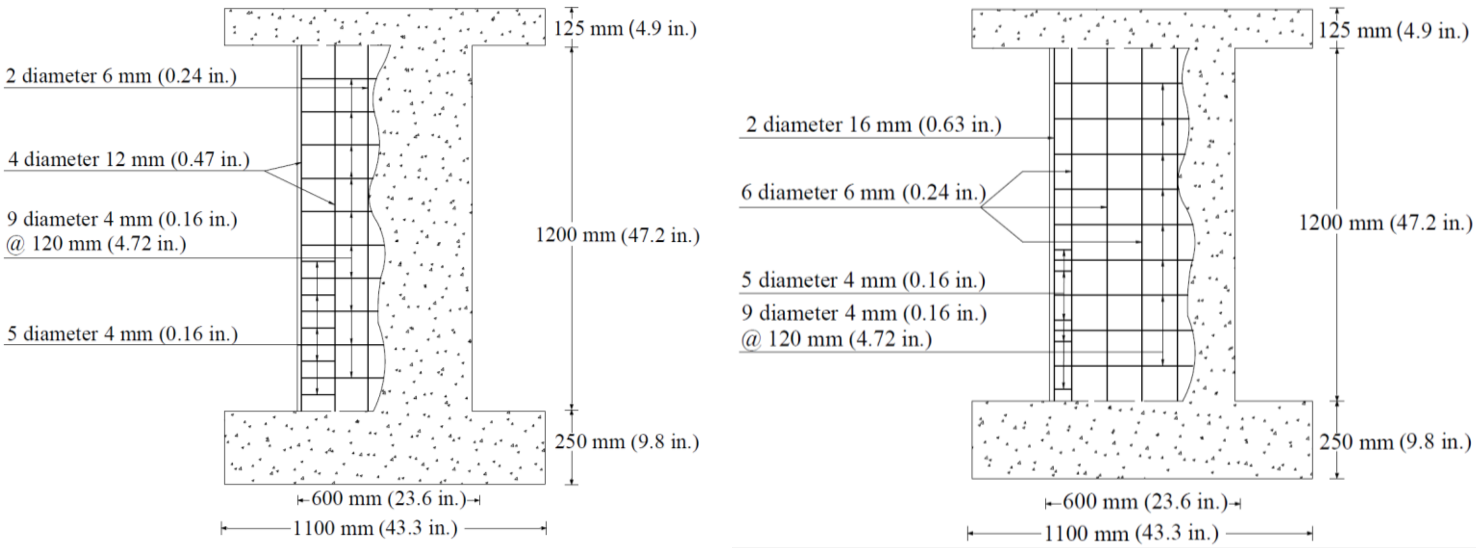

Elevation view of SW6 Elevation view of SW5

Fig. 2. Details of walls tested by Pilakoutas and Elnashai (1995)

Concrete material model

The wall concrete was modeled using the smeared crack Winfrith material model (MAT084 in LS-DYNA) (Broadhouse and Neilson 1987). Input parameters were modulus of elasticity, uniaxial compressive and tensile strength, crack width at which crack-normal tensile stress becomes zero and aggregate size (Schwer 2011). For this research, modulus of elasticity and the mean tensile strength were calculated following ACI 318-14 (ACI 2014) and fib (2013), respectively. Pilakoutas and Elnashai (1995) reported that the uncracked (elastic) stiffness was far greater than the stiffness observed in the test. Pilakoutas and Elnashai (1995) attributed this difference to loading conditions, material characteristics and curing conditions. In addition, restrained shrinkage cracks can play a role in the deviation of experimental stiffness from the elastic stiffness. To address this issue in FEA, a lower bound tensile strength equal to 70% of the mean tensile strength was used in the models, considering the large variability in tensile strength and the influence of shrinkage and curing on the initial stiffness. This value allowed a match of the initiation of tensile cracking and initial stiffness of walls between FEA and test results.

Post peak behavior in tension was approximated as linear. The crack width corresponding to zero crack-normal tensile stress is determined as $2G_f / f_t$, where G_f is the fracture energy of concrete estimated by fib (2013) and f_t is the uniaxial tensile strength of concrete.

In compression, concrete is approximated as elastic-perfectly plastic. Strength degradation due to crushing of concrete was accounted for explicitly using the element removal technique. Crushed elements were eroded to capture the post-peak strength degradation of structural walls. This was particularly important to simulate the behavior of SW5 that failed under shear. A principal compression strain based erosion criteria, shown to be effective in simulating walls under cyclic loading (Epackachi and Whittaker 2018), was utilized. Principal compression strain limit after which element removal took place was calibrated to be 0.040. The foundation was modeled using linear elastic concrete properties.

Reinforcing bar steel material model

Steel reinforcing bars were modeled using a piecewise linear plasticity model (MAT024 in LS-DYNA). Steel reinforcing bar material properties tested by Pilakoutas and Elnashai (1995) were used in the models (Fig. 3). Only a trilinear idealization of stress-strain relationship for steel bars was reported by Pilakoutas and Elnashai (1995) and was used in this study. Modulus of elasticity of all reinforcing bars was used as reported through tests: 200 GPa (29,000 ksi). Poisson's ratio was taken as 0.3. The rupture of reinforcing bars was captured by defining a limit on plastic strain based on the stress-strain curves for the steel rebar shown in Fig. 3. Reinforcement buckling was not considered.

Post-tensioning steel material model

Post-tensioning strands were modeled using cable discrete beam material (MAT071 in LS-DYNA), assuming elastic behavior. This assumption was validated by confirming that stresses in strands did not exceed the yield strength during analyses. The modulus of elasticity of strands was 196,500 MPa (28,500 ksi) per ACI 318-14 (ACI 2014). Post-tensioning strands were connected to the cap and foundation through rigid plates to avoid stress concentrations at anchorages.

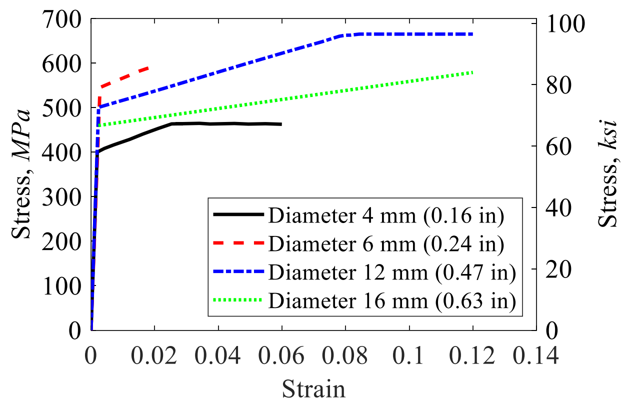

Fig. 3. Stress-strain relationship of the steel bars as tested by Pilakoutas and Elnashai (1995)

Finite elements

Concrete was modeled using eight node, single integration point, and continuum elements. Reinforcing bars were modeled using Hughes-Liu beams elements with cross section integration formulation, 4 integration points per cross section. Reinforcing bar elements were embedded in concrete elements using shared nodes, assuming perfect bond between steel and concrete. Post-tensioning strands were modeled using cable discrete beams that can only develop tension.

A smaller mesh size (10 mm (0.4 in.) x 10 mm (0.4 in.) x 15 mm (0.6 in.)) was used near the wall base where significant damage was expected. Near the top of the walls, in the foundation and in the cap beam, a coarser mesh (10 mm (0.4 in.) x 15 mm (0.6 in.) x 15 mm (0.6 in.)) was used. A mesh sensitivity analysis showed that the mesh size was adequate. Element aspect ratios were lower than 1.6 for all parts of the walls.

Loading and boundary conditions

A lateral cyclic displacement was applied on the elastic cap beam above the walls following the same loading protocol used in testing. All degrees of freedom on the bottom face of the foundation were restrained, simulating a fixed base.

Contact

For the original (pre-retrofit) walls, the walls and foundation nodes were merged together. For the retrofitted walls, to simulate the partial wall base and reinforcement cut in FEA, the shared nodes of concrete elements of the wall and the foundation were unmerged. Similarly, the shared nodes of reinforcing bars within the wall and within foundation were also unmerged. A surface-to-surface, mortar-based hard contact was defined between surfaces of the wall and the foundation. The friction coefficient was assumed to be 1.0 which is within the range recommended by ACI 318-14 (ACI 2014).

Comparison of FEA and Test Results of Original Walls

Load-displacement results obtained from the FEA and testing were compared to validate FEA. As described earlier, material properties used in the FEA were obtained through tests, ACI 318 or fib Model Code provisions (ACI 2014; fib 2013). The only properties that required calibration were the concrete tensile strength, and the concrete principal compression strain after which element removal was activated. In reporting results throughout the paper, unless otherwise indicated, all results are reported as the average values of interest in the positive and negative displacement directions.

Comparison of FEA and test results for wall SW6

Wall SW6 was reported to have failed under a combination of shear and flexure. Force-displacement diagrams for SW6 predicted by the FEA and measured by testing are compared in Fig. 4(a). In general, there is an acceptable agreement between the FEA and test results in terms of stiffness and strength. After the ninth loading cycle (1.67% lateral drift ratio), strength predicted by the FEA was up to 22% lower than the one measured by testing. The difference is explained by the fact that a vertical web bar fracture was predicted by the FEA at this cycle but was not observed in testing. The fracture in the FEA may have been caused by the trilinear idealization of steel stress-strain behavior. It may also have been caused by the inherent variation in steel material properties between test coupons and the reinforcement used in the walls, since the bar fractured in the FEA was the 6 mm (0.24 in.) diameter bar with significantly lower ultimate strain than other bars from the coupon tests (Fig. 3). FEA underestimated the pinching effects and over-estimated energy dissipation particularly at larger displacement cycles. This is also attributed to the tri-linear approximation used in modeling steel reinforcement stress-strain behavior.

Comparison of FEA and test results for wall SW5

Wall SW5 was reported to have failed under shear during testing. Force-displacement diagrams predicted by FEA and measured by tests are shown in Fig. 4(b) for wall SW5. There is an acceptable agreement between FEA and test data in terms of strength and stiffness. For the last two cycles (drift ratios of 1.8% and 2.2%), the strength, residual displacement and energy dissipation were under-estimated by FEA. The maximum error in strength was 20% and was deemed acceptable given uncertainties in material properties and specimen geometry.

Overall, finite element models captured the failure mechanism, damage states, displacements at which bar yielding and fracture occurred with reasonable accuracy as compared to the experimentally reported ones. Table 1 compares first yielding, first fracture of vertical reinforcing bars and fracture of transverse reinforcing bars obtained from the FEA with the experimental observations for walls SW6 and SW5. The events of interest happened within the same cycle or a cycle earlier in the FEA when compared to experimental testing, except vertical reinforcing bar fracture in SW6, where FEA predicted failure while it was not observed in testing.

Table 1. Failure sequence comparison

Wall	Vertical bar yielding	Vertical bar fracture	Transverse bar fracture
SW6 (Test)	0.33%-0.50% drift	None reported	1.33%-1.50% drift
SW6 (FE model)	0.33%-0.50% drift	1.50%-1.67% drift	1.33%-1.50% drift
SW5 (Test)	0.50%-0.67% drift	None reported	1.17%-1.33% drift
SW5 (FE model)	0.33%-0.50% drift	No fracture	0.83%-1.00% drift

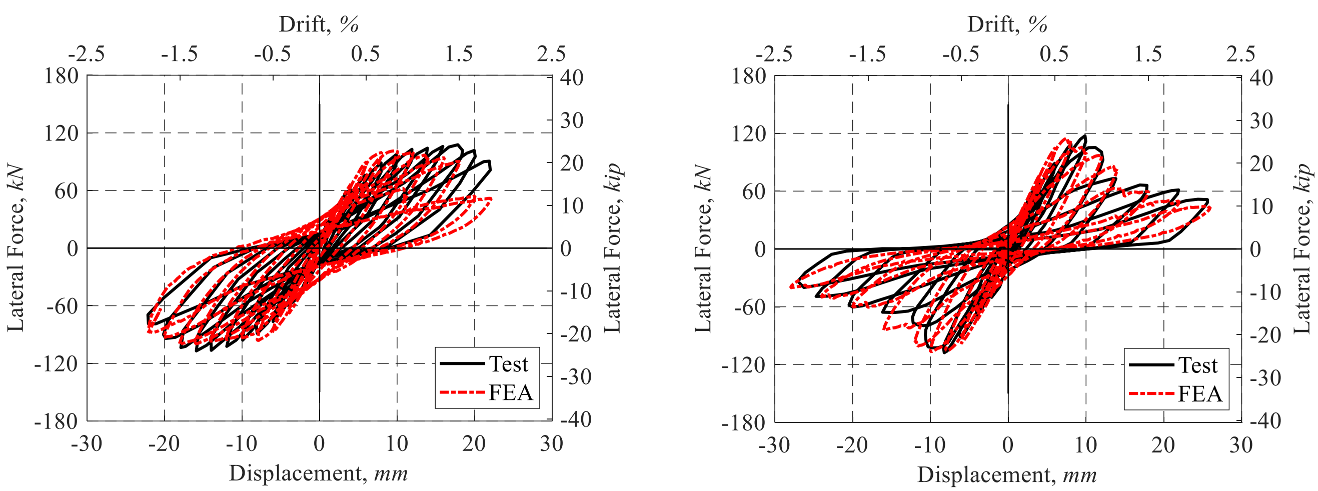

(a) (b)

Fig. 4. Comparison of force-displacement from FEA and tests for SW6 (a) and SW5 (b)

Preliminary Selection of Retrofit Parameters

The proposed retrofit strategy is composed of two steps: Step 1) weakening of walls by cutting a number of vertical bars and partially cutting the wall base at the foundation interface, and Step 2) self-centering by adding unbonded post-tension strands. The retrofit parameters include the amount of mild steel reinforcement to be cut, length of the cut, amount of post-tensioning force and confinement details.

The amount of reinforcement to be cut, as part of weakening strategy, can be determined based on the desired level of strength and stiffness reduction, desired self-centering ability and by practical considerations. For example, for walls SW6 and SW5, cutting only the outermost single layer of reinforcement bars resulted in 56% and 26% of the original wall reinforcement (as shown by the sketch in Fig. 5(a)). Wall base was cut from the wall edge to halfway between the cut and uncut vertical rebar. Kurama (2002) recommended that for post-tensioned rocking walls in high seismic regions, vertical reinforcement should be at least 50% of the one in an equivalent emulative wall. Designers may follow this recommendation where possible. Wall SW6 satisfied the recommendation by Kurama (2002). Wall SW5 did not follow this recommendation with 26% of the original reinforcement amount. For this case, the amount of initial post-tensioning force can be selected considering energy dissipation using the minimum required relative-energy dissipation ratio of ACI ITG-5.2-09 (ACI 2009).

The amount of post-tensioning was studied as a variable in this paper for SW6 and SW5. The following simplified procedure can also be used to determine the initial post-tension amount, given a desired wall base cut length and a desired amount of strength recovery: 1) Axial load-moment (P-M) interaction curves are built for original and weakened walls. 2) Based on the desired lateral moment strength recovery amount, the required axial load for the weakened wall is calculated from the P-M interaction curve. This axial load is approximately the amount of post-tensioning when the wall is reaching its moment capacity (when strands are elongated). 3) To identify the initial post-tensioning amount needed, increase in the length of strands is determined by calculating rotation and curvature across the wall height. Initial post-tensioning force is determined by subtracting this increase in post-tensioning force from the force determined from the P-M interaction curve. Note that the post-tensioning tendons are designed to remain elastic at the design drift.

FEA Results of the Retrofitted Walls

For both walls (SW6 and SW5), the effects of cutting the wall base on strength, stiffness, energy dissipation and residual displacements were studied. Wall base was cut so that one outermost pair of reinforcement on each side of the wall was cut. This resulted in 56% (SW6) and 26% (SW5) of the reinforcement and 67% (SW6) and 86% (SW5) of the wall base length to be left uncut.

Self-centering was added to the weakened walls through post-tensioning strands. A parametric study was conducted to understand the effects of the level of initial post-tensioning force and the location of post-tensioning strands on the wall behavior and to identify the details of promising retrofit schemes. The initial post-tension force was varied as $0.25F_{py}$, $0.50F_{py}$, and $0.75F_{py}$, where F_{py} denotes the yield strength of the post-tensioning strands taken as 90% of the ultimate strength per ACI 318-14 (ACI 2014). The cross-sectional area of each strand was 92.9 mm^2 (0.144 in^2). Post-tension strand area was not a parameter, as strands did not reach their yield strength in this study. For cases with one strand on each side of the wall, concentrically placed along the length of the wall, this led to the initial post-tensioning force levels of $0.06A_gf'_c$, $0.11A_gf'_c$ and $0.17A_gf'_c$ for wall SW6 and correspond to $0.07A_gf'_c$, $0.14A_gf'_c$ and $0.20A_gf'_c$ for wall SW5. Here, A_g is the cross sectional area of walls, f'_c is the concrete compressive strength, and $A_gf'_c$ is the wall axial load capacity.

The location (eccentricity and number) of strands was varied by placing two strands on each side of the wall eccentrically across the length of the wall. Three different eccentricities with respect to the mid-length of wall were investigated: $0.00l_w$, $0.10l_w$, and $0.29l_w$, where l_w is the wall length.

When investigating eccentricity, the initial post-tensioning stress was kept at $0.25F_{py}$ on each of the two strands on each side of the wall.

The FEA results of retrofitted walls and original walls were compared in terms of load-displacement curves. Results were also compared in terms of four criteria: relative energy-dissipation ratio, lateral strength, residual displacement and secant stiffness per cycle. Relative energy-dissipation ratio per cycle was calculated using the ratio of the area under the closed loops of the force-displacement diagrams for each cycle of loading to the area of the circumscribing parallelograms generated from the initial stiffness of the wall. ACI ITG-5.2-09 (ACI ITG 2009) requires unbonded post-tensioned walls to have a minimum relative energy-dissipation ratio of 0.125. Residual displacement was calculated as the displacement upon unloading when the lateral force drops to zero. Secant stiffness was calculated as the lateral force at the maximum displacement in each cycle divided by the maximum imposed displacement in the associated cycle. It should be noted that maximum force may not always occur at the maximum displacement when using this definition of secant stiffness. Finally, crack patterns and principal strain contour plots of walls of retrofitted and original walls were compared to understand failure modes.

Retrofit for wall SW6

Fig. 5 compares the hysteretic behavior of the original and the retrofitted wall for varying post-tensioning forces applied at $0.00l_w$ eccentricity. Fig. 6 compares the original and retrofitted walls in terms of energy dissipation, lateral strength, residual displacement and secant stiffness.

Post-tensioning at $0.06A_gf'_c$, $0.11A_gf'_c$ and $0.17A_gf'_c$ was shown to result in 68%, 95% and 98% of the lateral strength of the original wall, on average, respectively, partially or fully recovering the strength loss due to weakening. The initial post-tensioning force needed to restore SW6 strength to 95% of the original capacity can also be predicted by the preliminary analysis method described earlier. FEA and preliminary analysis predictions were within 24% of each other. This error in the preliminary analysis is deemed acceptable.

In general, residual displacements decreased since strands can provide self-centering at the wall base.

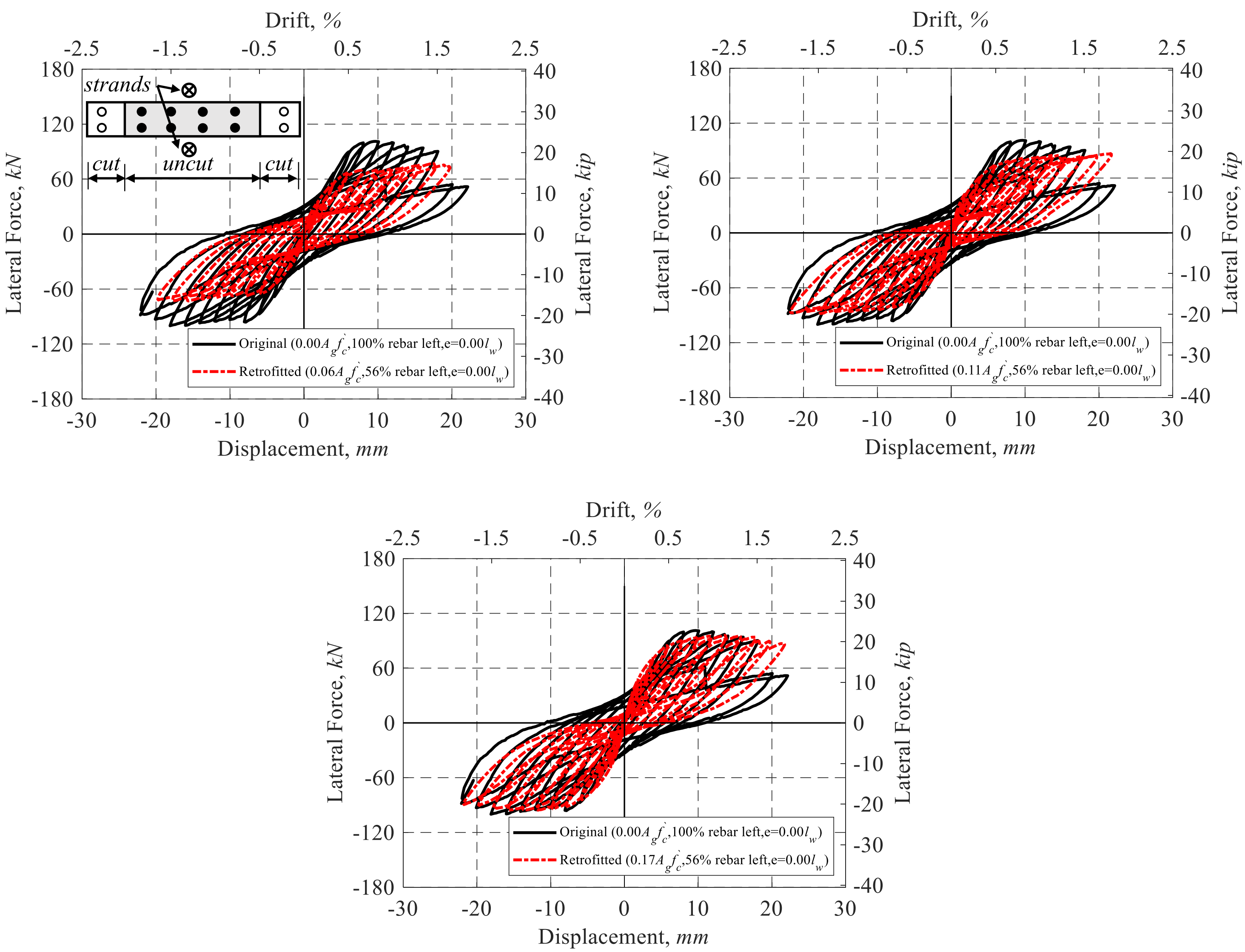

Fig. 5. Comparison of force-displacement of the original and retrofitted SW6 for varying post-tension levels.

For the varying post-tension forces applied concentrically, the average of the residual displacement ratio of the retrofitted wall to the original wall ranged between 1.23 and 0.57. The increase in residual displacements was caused by the effects of weakening overcoming the effects of smaller amount of post-tension on residual displacements. However, this increase occurred at very small drifts (i.e., the first 3 cycles in which the drift is less than 0.5%) and is not significant to the overall behavior of the walls.

Relative energy-dissipation ratio of the retrofitted walls was smaller than the one of the original walls under all initial post-tension force levels, due to the reduced residual displacements or lateral strength. The increase in the initial post-tensioning force from $0.06A_gf'_c$ to $0.17A_gf'_c$ resulted in a reduction in relative energy-dissipation ratio per cycle from 95% to 66% of the original wall, on average across all loading cycles.

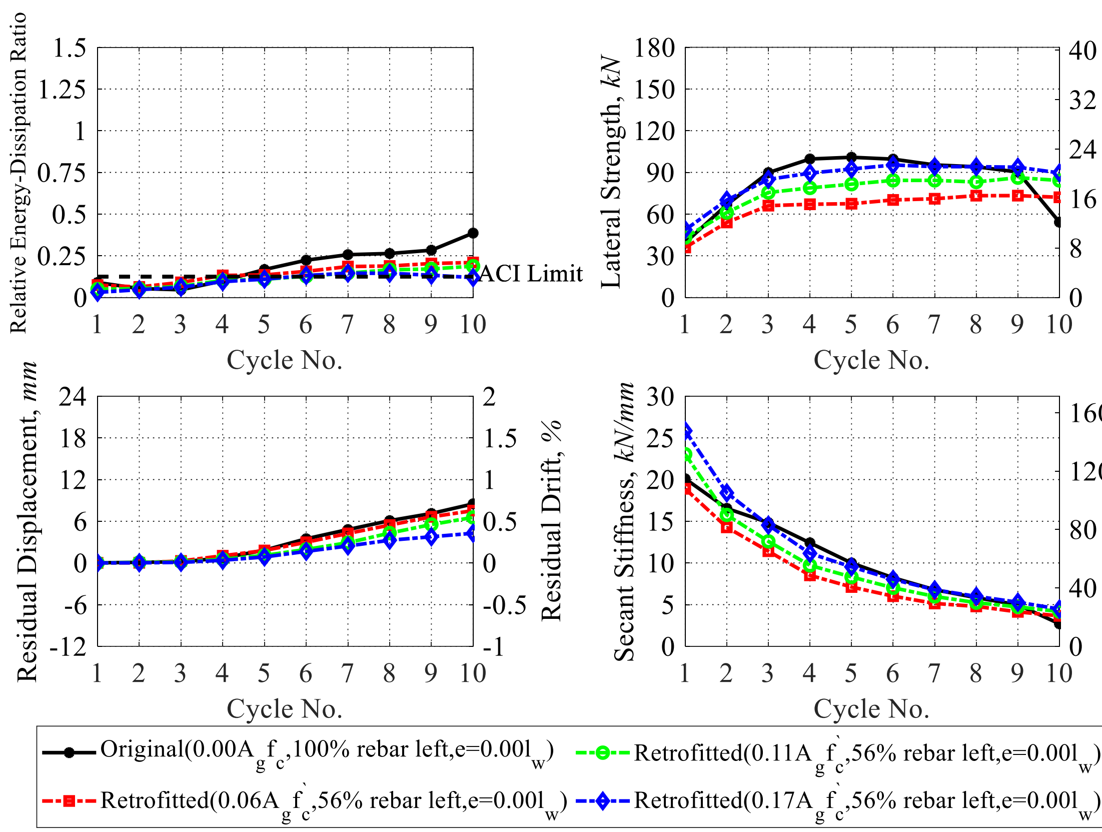

Fig. 6. Comparison of relative energy-dissipation ratio, lateral strength, residual displacement and secant stiffness per cycle for the original and retrofitted SW6 for varying post-tension levels.

The secant stiffness was entirely recovered by the addition of post-tensioning, due to the increase in strength. The secant stiffness grew with increasing post-tension force levels. The initial post-tensioning of 0.11$A_g f'_c$ was considered for the rest of the study as a level of post-tensioning force that can recover loss of strength due to weakening and that can reasonably balance energy dissipation and residual displacements. This enabled a comparison of an original and retrofitted wall with similar strengths and stiffness but different expected failure mechanisms.

Fig. 7 shows the effect of location of post-tensioning strands in terms of relative energy-dissipation ratio, lateral strength, residual displacement and secant stiffness per cycle. The eccentricity, e, is also shown on the sketch.

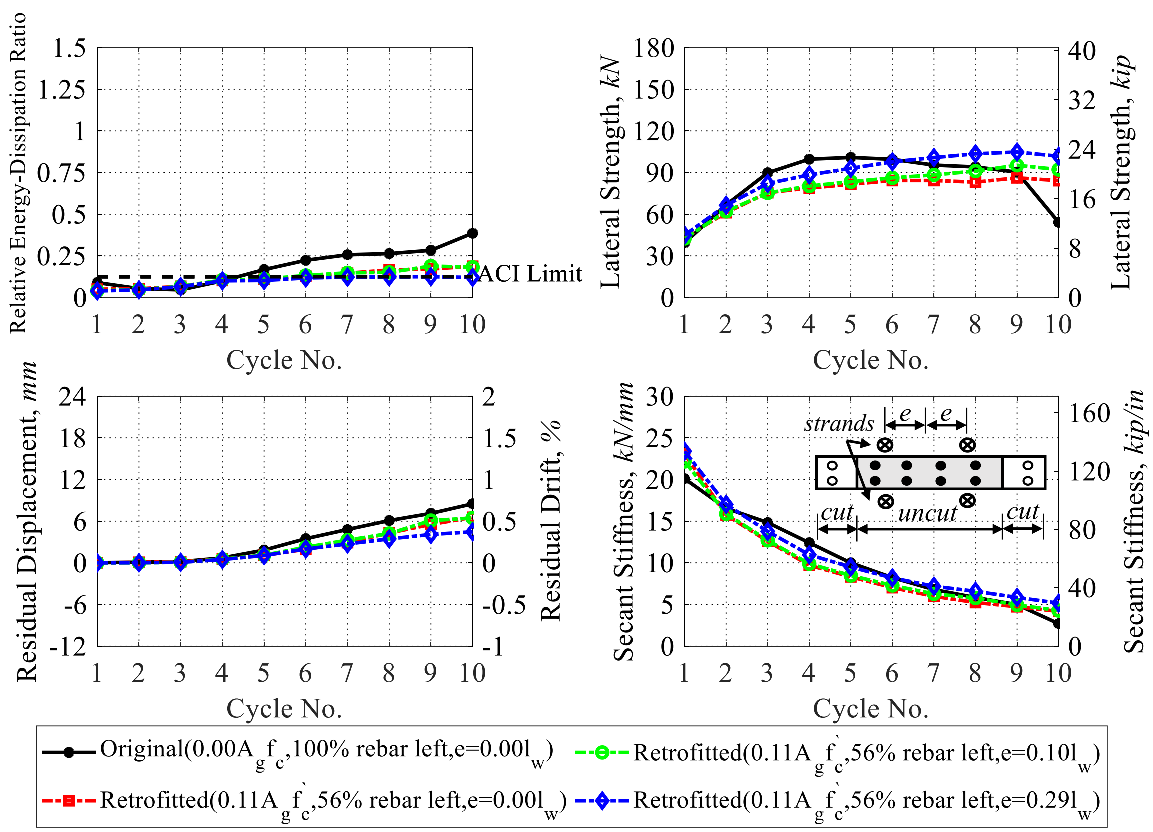

Fig. 7. Effect of location of post-tensioning strands in terms of relative energy-dissipation ratio, lateral strength, residual displacement and secant stiffness for SW6

Placing post-tensioning strands with the eccentricities of $0.00l_w$, $0.10l_w$ and $0.29l_w$ yielded retrofitted walls with 95%, 100%, and 110% of the lateral strength of the original wall, respectively. The other criteria of interest were not sensitive to the location of post-tensioning strands. Based on these results, strands were decided to be placed concentrically. This placement also helps control stresses and post-tension losses in strands under lateral displacements.

Retrofit for wall SW5

For new construction, the toes of self-centering walls need to be confined well to prevent premature crushing of the toe (ACI ITG 2009; Kurama 2002). Addition of post tensioning to SW5 caused more than 40% of the elements near the wall toes to crush and erode. Analysis stopped after 0.67% drift due to a 63% drop in strength. To prevent the premature failure of concrete in the compression zone, the retrofit strategy includes confinement of wall toes, when needed (i.e. for all analyses conducted on retrofitted SW5). For SW5, a C-shaped steel plate with a thickness of 6.35 mm (0.25 in) and yield strength of 413.7 MPa (60 ksi) was placed across the cut portion of the wall base. The steel confinement plate was selected such that it remained elastic during the loading history. The steel confinement plate was modeled using 8-node, single integration point, continuum elements and was connected to the concrete elements of the wall and the foundation with surface-to-surface contact.

Fig. 8 shows the force-displacement diagram of the retrofitted wall with varying post-tensioning forces. Fig. 9 compares the original and retrofitted walls in terms of the criteria of interest. Similar to SW6, for SW5, the addition of post-tension increased the strength of the weakened wall. By post-tensioning strands to $0.07A_gf'_c$, $0.14A_gf'_c$ and $0.20A_gf'_c$, the retrofitted wall had 69%, 82% and 90% of the lateral strength of the original wall, on average, respectively. When the initial post-tensioning force in SW5 that leads the strength to be 82% of the original capacity was predicted by the preliminary analysis described earlier, the prediction was within 23% of the FEA prediction. This is an acceptable level of error for preliminary analysis.

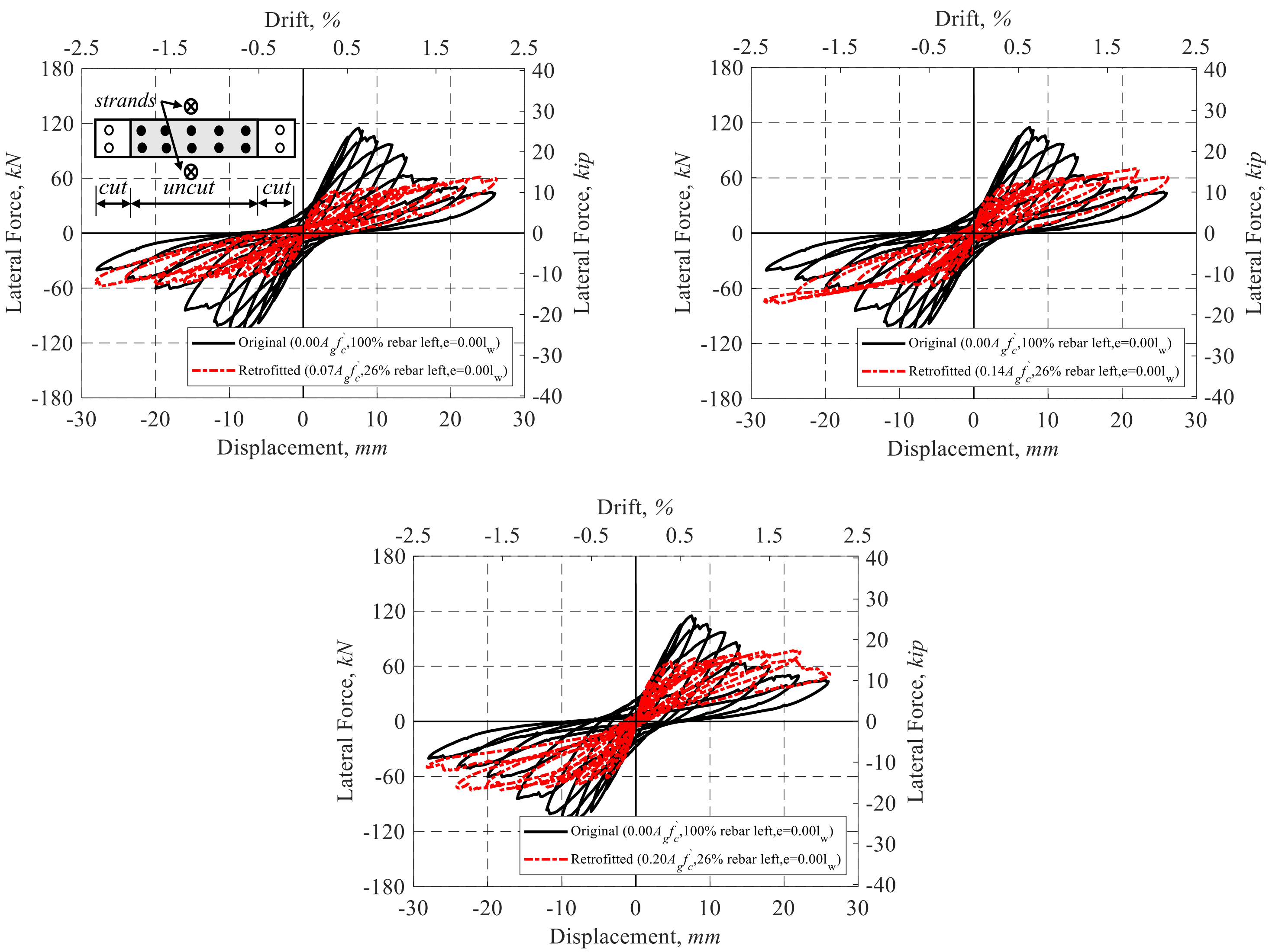

Fig. 8. Comparison of force-displacement of the original and retrofitted SW5 for varying post-tension levels

Post-tensioning decreased residual displacements in weakened walls, a conclusion drawn earlier for SW6. For the levels of post-tensioning considered in the parametric study, the average residual displacement ratio of the retrofitted wall to the original wall ranged between 1.32 and 0.38. The increase in residual displacements occurred at very small drifts (i.e. less than 0.5%) and is not significant to the overall behavior of the walls.

Relative energy-dissipation ratio in the retrofitted wall was between 92% (with post-tensioning equal to 0.20$A_g f'_c$) and 120% (with post-tensioning equal to 0.14$A_g f'_c$) of that of the original wall, on average. However, from the fifth cycle to end, the relative energy-dissipation ratio of the retrofitted wall was less than the original wall, yet satisfying ACI ITG-5.2-09. Lower energy dissipation at high post-tension levels was due to earlier concrete crushing, followed by a higher post-tension loss, compared to the low post-tension levels.

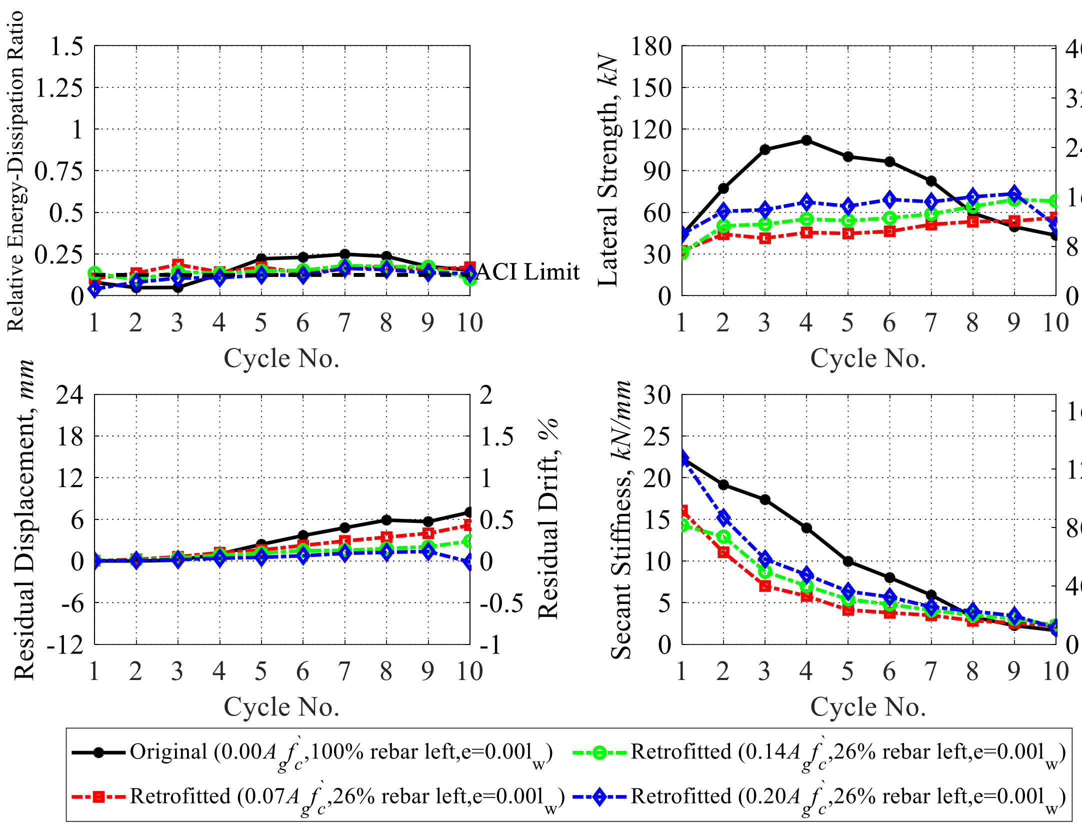

Fig. 9. Comparison of energy dissipation, lateral strength, residual displacement and secant stiffness per cycle for the original and retrofitted SW5 for varying post-tension levels.

The secant stiffness of the retrofitted walls varied between 69% and 89% of the original wall with increasing post-tensioning forces. Based on these results, and its balancing effects on strength and residual displacement, $0.14A_g f`_c$ of post-tensioning was selected to be used for the retrofit of SW5. This allowed a comparison of the failure mechanism of the original wall to the retrofitted wall with a smaller strength and stiffness.

Fig. 10 shows a comparison of relative energy-dissipation ratio, lateral strength, residual displacement, and secant stiffness for the walls retrofitted with varying post-tension eccentricities. Similar to SW6, lateral strength was the criterion most sensitive to eccentricity of post-tensioning. Concentrating post-tensioning strands at $0.00l_w$, $0.10l_w$ and $0.29l_w$ enabled the system to reach 82%, 93% and 113% of the lateral strength of the original wall, respectively.

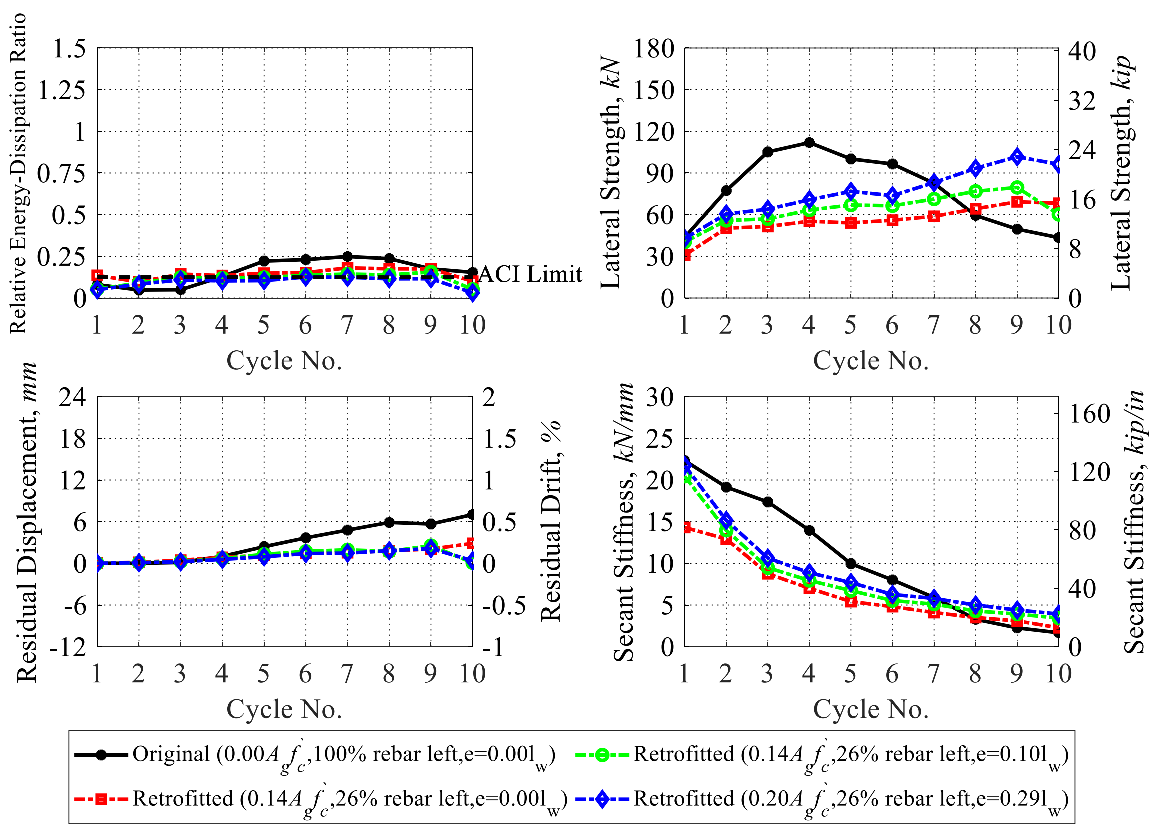

Fig. 10. Effect of location of post-tensioning strands in terms of energy dissipation, lateral strength, residual displacement and secant stiffness for SW5

Failure Modes of Original and Retrofitted Walls

To understand failure modes, the followings were compared for the original and retrofitted walls: 1) contour plots of principal compression strains, tension strains and crack patterns; 2) failure sequence of wall components. Strain contours are presented at the drift ratios when the walls were reported to have failed, and at approximately half the failure drift ratio (closer to a design earthquake displacement). Strain contour plots and crack maps also provide information on the expected damage state and spread of damage, which can be indicators of reparability and seismic resiliency. Failure sequence of wall components is an indicator for failure modes.

For comparisons, the area of reinforcement left uncut and the post-tension levels were the ones identified as optimal based on the comparisons presented previously. These were 56% of uncut reinforcement and concentrically placed post-tension equal to $0.11A_gf'_c$ for SW6, and 26% of uncut reinforcement and concentrically placed post-tension equal to $0.14A_gf'_c$ for SW5.

Strain contours and crack patterns

Fig. 11 shows the principal compression and tension strain contours together with crack patterns at drift ratios of 0.9% and 1.8% (drift ratio at the failure of the original wall) for the retrofitted and the original wall for SW6. Principal compression strains show that fewer concrete elements crushed in a smaller area for the retrofitted wall than the original wall, and these elements concentrated near the weakened section (wall base). Principal tensile strain contours together with the crack patterns show that cracking is less intense and concentrated near the weakened section for the retrofitted wall as compared to the original wall.

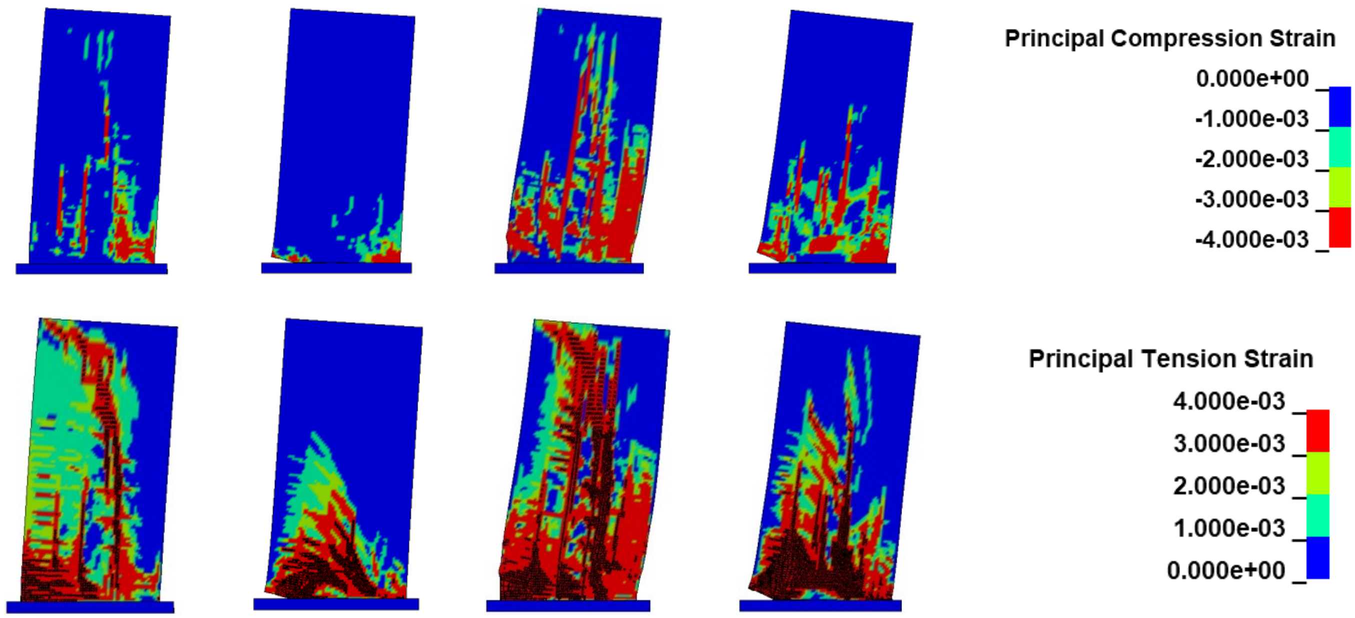

Original, 0.9%   Retrofitted, 0.9%   Original, 1.8%   Retrofitted, 1.8%

Fig. 11. Principal compression and tension strain contours for the original and retrofitted SW6 at different drift ratios.

Fig. 12 shows principal compression and tension strain contours together with crack patterns at drift ratios of 1.0% and 2.2% (drift ratio at the failure of the original wall) for the original and retrofitted walls for SW5. White regions in contour plots indicate removal of concrete elements due to crushing. The conclusions are the same as the ones drawn for SW6.

Failure sequence of wall components

Important events leading to the failure of the walls are considered to be the first yielding of a vertical bar in flexure, the first fracture of a vertical reinforcing bar in flexure, the first yielding of a transverse reinforcing bar, the first fracture of a transverse reinforcing bar in shear and crushing of concrete. In order to provide a quantitative means of comparison for concrete crushing, the volumetric percentage of crushed concrete finite elements (i.e., elements reaching the principal compression strain of 0.003 (for SW6, SW5) for unconfined concrete, and 0.0078 (for SW6) and 0.0065 (for SW5) for confined concrete, respectively) was recorded. Strains associated with the crushing of confined concrete were extracted from Pilakoutas and Elnashai (1995). Fig. 13 summarizes the failure sequence of wall components for the original and the retrofitted walls.

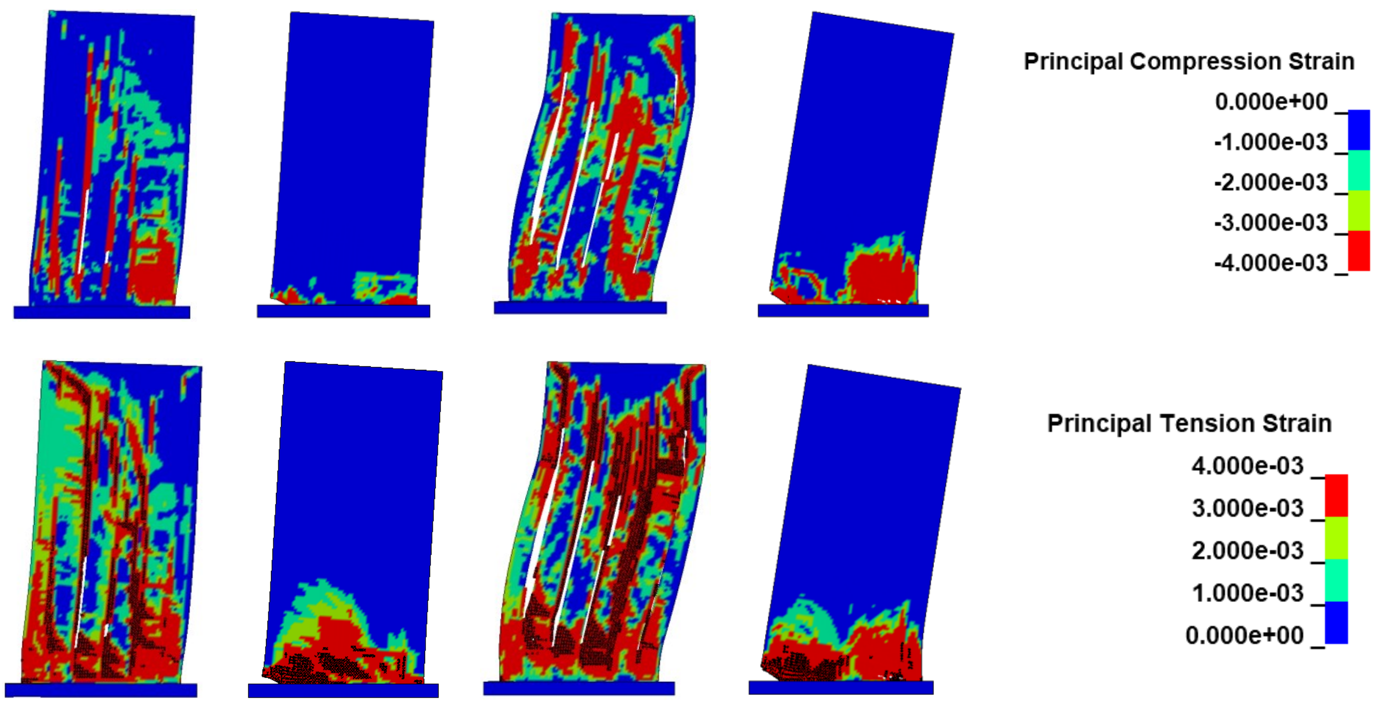

Original, 1.0%   Retrofitted, 1.0%   Original, 2.2%   Retrofitted, 2.2%

Fig. 12. Principal compression and tension strain contours for the original and retrofitted SW5 at different drift ratios.

For SW6, the first flexural yield of flexure reinforcement was delayed from the third (drift ratio of 0.33% to 0.50%) to the seventh (drift ratio of 1.00% to 1.18%) loading cycle due to retrofit. The retrofit allowed the first stirrup fracture to be delayed to the last loading cycle. On the other hand, the first flexure reinforcement fractured earlier for the retrofitted wall because the reinforcing bar with the diameter of 6 mm (0.24 in.) had very little ductility compared to the other bars (Fig. 3). The outermost layer of reinforcement in the original wall (12 mm (0.47 in.)) had a much higher ductility than this bar, delaying fracture. The volumetric percentage of crushed concrete elements in the boundary region was considerably less in the retrofitted wall than that of original wall, showing the efficiency of the retrofit method in limiting damage in terms of concrete crushing.

For SW5, the retrofit caused the first flexural reinforcing bar to yield and fracture earlier than it did for the original wall. This can be explained by the fact that the vertical rebar with the diameter of 16 mm (0.63 in.) was cut for the retrofit, leaving the lowest ductility 6 mm diameter (0.24 in.) bars (Fig. 3) to be the closest to the highest tension side. Conversely, the first stirrup fractured during the seventh cycle of loading in the original wall, while for the retrofitted wall, no bar fracture was observed, indicating a shift away from a shear dominated failure. The volumetric percentage of the crushed concrete in the web decreased from 24% to 10% in the retrofitted wall.

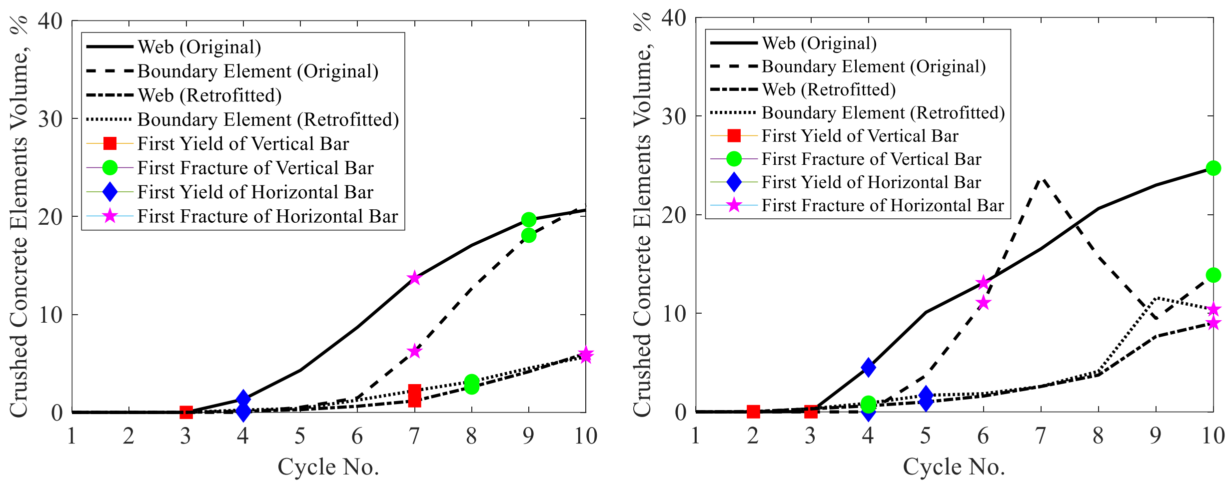

(a) (b)

Fig. 13. Failure sequence for SW6 (a) and SW5 (b)

Summary and Conclusions

Concepts of self-centering developed for newly built, flexure-dominant RC shear walls have been extended to a retrofit strategy in this study. This retrofit strategy combined weakening through a wall base cut and self-centering through unbonded post-tension strands. Unlike newly built self-centering walls that are designed for flexure failures, the retrofit strategy focused on poorly designed shear walls that are expected to have partial (flexure-compression through core crushing) or full shear (diagonal cracks near wall mid-height) failures. Some of the conclusions of this study were consistent with the ones of studies on newly built self-centering walls.

The retrofit was evaluated through validated FEA for RC shear walls with outdated seismic design details. Two slender, non-code compliant shear walls were analyzed before and after retrofit. The conclusions drawn from the analyses are as follows:

- An acceptable correlation was achieved between FEA and test results. Two parameters that required calibration were the concrete tensile strength and strain of concrete after which element removal was activated. The other input parameters were as obtained from testing or as specified by design codes.
- Adding post-tensioning to walls enabled the recovery of the loss of strength and secant stiffness caused by weakening. Strength and secant stiffness of the retrofitted walls were 69% to 98% and 69% to 100% of the original walls, respectively. The retrofit method with two distinct steps (base cut and post-tensioning), that have the opposite effects on strength and secant stiffness, allows engineers to tailor strength and self-centering to their needs.
- Although compared to the original walls, the retrofit strategy decreased energy dissipation, the reduced energy dissipation was shown to be sufficient per ACI ITG-5.2-09 (ACI ITG 2009). Residual displacements were also reduced by the retrofit. Applying post-tensioning beyond 11% to 14% of the axial load capacity of the walls did not reduce the residual displacements further and is not recommended.
- The increase of post-tensioning force increased lateral strength. However, high post-tension also increases concrete crushing. For this reason, post-tension levels recommended were identified to be between 11% and 14% of the axial capacity of the walls. Steel confinement provided at the weakened edges of the wall was shown to be effective in delaying concrete crushing and is recommended.

- A simplified approach to estimate the amount of initial post-tensioning force, for a given base length cut and desired strength after retrofit, was proposed for preliminary design.
- Eccentricity of post-tensioning strands across the length of the walls did not alter secant stiffness, residual displacements, or energy dissipation considerably and increased strength in small amounts. For these reasons, concentric post-tensioning is recommended.
- The retrofit decreased the spread of cracking over the walls. Cracks became concentrated near the weakened section by the base of the wall. There were no shear cracks across the height of the walls after retrofit, beyond the wall base.
- The retrofit decreased the number of crushed concrete elements in both boundary regions and web of the walls. Overall, the contour plots of principal tension and compression strains indicated that the damage was confined to the base of the wall, and flexural yielding had a higher contribution to the failure mode.
- Fracture of the transverse reinforcement is delayed by the retrofit, indicating that the shear contribution to failure decreased. For the walls selected from the literature, vertical bars in flexure of the retrofitted walls ruptured earlier than they did for the original walls. This may be due to the insufficient ductility of the uncut rebar used in these specific walls or the fact that the flexural contribution to failure was increased.
- Overall, the results showed that retrofit strategy can reduce the contribution of shear to the global response of code-deficient RC walls.

Baseline walls investigated in this study did not have any axial load, consistent with the walls for which test data was available. Although this study targeted walls that do not carry significant gravity loads (FEMA building type C2 according to FEMA 454 (FEMA 2006)), lack of axial load is a limitation of the study. Addition of axial load to walls may change the response of the retrofitted walls, in ways similar to the impact of additional post tensioning.

This study only investigated the impacts of retrofit on the behavior of isolated wall components. When considering this retrofit technique, the impact of changes in wall behavior on the surrounding structural and non-structural elements should also be checked, particularly for displacement and energy dissipation demands of these elements. System analyses were out of the scope of this paper.

Acknowledgements

This material is based upon work supported by the National Science Foundation under Grant No. 1663063. Any opinions, findings, and conclusions or recommendations expressed in this material are those of the authors and do not necessarily reflect the views of the National Science Foundation.

References

ACI (American Concrete Institute). (1971). "Building code requirements for reinforced concrete" Farmington Hills, MI.

ACI (American Concrete Institute). (2014). "Building code requirements for structural concrete (aci 318-14): Commentary on building code requirements for structural concrete (aci 318r-14)" *ACI 318-14,* Farmington Hills, MI.

ACI ITG (American Concrete Institute). (2009). "Requirements for design of a special unbonded post-tensioned precast shear wall satisfying aci itg-5.1 and commentary" *ACI ITG-5.2-09,* Farmington Hills, MI.

Antoniades, K. K., Salonikios, T. N., and Kappos, A. J. (2003). "Cyclic tests on seismically damaged reinforced concrete walls strengthened using fiber-reinforced polymer reinforcement." *ACI Struct J*, 100(4), 510-518.

ASCE (American Society of Civil Engineers). (2017). "Seismic evaluation and retrofit of existing buildings: Asce/sei, 41-17" Reston, VA.

Broadhouse, B. J., and Neilson, A. J. (1987). "Modelling reinforced concrete structures in dyna3d." *Rep. AEEW-M-2465,* UKAEA Atomic Energy Establishment, U.K.

Christidis, K. I., Vougioukas, E., and Trezos, K. G. (2016). "Strengthening of non-conforming rc shear walls using different steel configurations." *Eng. Struct.*, 124, 258-268.

Elnashai, A. S., and Pinho, R. (1998). "Repair and retrofitting of rc walls using selective techniques." *J. Earthq. Eng.*, 2(4), 525-568.

Epackachi, S., and Whittaker, A. S. (2018). "A validated numerical model for predicting the in-plane seismic response of lightly reinforced, low-aspect ratio reinforced concrete shear walls." *Eng. Struct.*, 168, 589-611.

FEMA (Federal Emergency Management Agency). (1998). "Fema 306: Evaluation of earthquake damaged concrete and masonry wall buildings: Basic procedures manual" Redwood City, CA.

FEMA (Federal Emergency Management Agency). (2006). "Fema 454: Designing for earthquakes: A manual for architects" US Department of Homeland Security, Washington, DC.

fib (federation internationale du beton). (2013). "Fib model code for concrete structures 2010"

Fiorato, A. E., Oesterle, R. G., and Corley, W. G. (1983). "Behavior of earthquake resistant structural walls before and after repair." *J. Proc.*, 80, 403-413.

Henry, R. S., Aaleti, S., Sritharan, S., and Ingham, J. M. (2010). "Concept and finite-element modeling of new steel shear connectors for self-centering wall systems." *J. Eng. Mech.*, 136(2), 220-229.

Holden, T., Restrepo, J., and Mander, J. B. (2003). "Seismic performance of precast reinforced and prestressed concrete walls." *J. Struct. Eng.*, 10.1061/(ASCE)0733-9445(2003)129:3(286), 286-296.

Ireland, M., Pampanin, S., and Bull, D. "Experimental investigations of a selective weakening approach for the seismic retrofit of rc walls." *Proc., New Zeal. Soc. Earthquake Eng. 2007 Annual Conf.*

Kam, W., and Pampanin, S. "Selective weakening techniques for retrofit of existing reinforced concrete structures." *Proc., 14th World Conf. on Earthquake Engineering (14WCEE)*.

Kam, W., and Pampanin, S. (2010). "Experimental and numerical validation of selective weakening retrofit for existing non-ductile rc frames." *Improving the seismic performance of existing buildings and other structures*, 706-720.

Kam, W. Y., and Pampanin, S. (2011). "The seismic performance of rc buildings in the 22 february 2011 christchurch earthquake." *Struct Concrete*, 12(4), 223-233.

Khalil, A., and Ghobarah, A. (2005). "Behaviour of rehabilitated structural walls." *J. Earthq. Eng.*, 9(3), 371-391.

Kurama, Y. (2002). "Hybrid post-tensioned precast concrete walls for use in seismic regions." *PCI J.*, 47, 36-59.

Lee, W., Jeong, H., Billington, S., Mahin, S., and Salkai, J. "Post-tensioned structural concrete bridge piers with self-centering characteristics." *Proc., Structural Engineering Research Frontiers Session of the 2007 Structures Congress*.

Lefas, I., and Kotsovos, M. (1990). "Strength and deformation characteristics of reinforced concrete walls under load reversals." *Struct. J.*, 87(6).

Lombard, J., Lau, D. T., Humar, J. L., Foo, S., and Cheung, M. S. "Seismic strengthening and repair of reinforced concrete shear walls." *Proc., 12th World Conf. on Earthquake Engineering*, 1-8.

LSTC. 2017. Ls-dyna keyword user's manual, version 971 R 9.0, Livermore, CA, Livermore Software Technology Corporation.

Marriott, D., Pampanin, S., and Palermo, A. (2009). "Quasi-static and pseudo-dynamic testing of unbonded post-tensioned rocking bridge piers with external replaceable dissipaters." *Earthq. Eng. Struct. D.*, 38(3), 331-354.

Nakaki, S., Stanton, J., and Sritharan, S. (1999). "Overview of the presss five-story precast test building." *PCI J.*, 44, 26-39.

Ou, Y.-C., Chiewanichakorn, M., Aref, A. J., and Lee, G. C. (2007). "Seismic performance of segmental precast unbonded posttensioned concrete bridge columns." *J. Struct. Eng.*, 10.1061/(ASCE)0733-9445(2007)133:11(1636), 1636-1647.

Palermo, A., Pampanin, S., and Marriott, D. (2007). "Design, modeling, and experimental response of seismic resistant bridge piers with posttensioned dissipating connections." *J. Struct. Eng.*, 10.1061/(ASCE)0733-9445(2007)133:11(1648), 1648-1661.

Pampanin, S. (2006). "Controversial aspects in seismic assessment and retrofit of structures in modern times: Understanding and implementing lessons from ancient heritage." *New Zeal. Soc. Earthquake Eng.*, 120-133.

Paterson, J., and Mitchell, D. (2003). "Seismic retrofit of shear walls with headed bars and carbon fiber wrap." *J. Struct. Eng.*, 10.1061/(ASCE)0733-9445(2003)129:5(606), 606-614.

Pilakoutas, K. (1990). "Earthquake resistant design of reinforced concrete walls." PhD thesis, Univ. of London, London.

Pilakoutas, K., and Elnashai, A. (1995). "Cyclic behavior of reinforced concrete cantilever walls, part i: Experimental results." *ACI Struct J*, 92(3), 271-281.

Pollino, M., and Bruneau, M. (2007). "Seismic retrofit of bridge steel truss piers using a controlled rocking approach." *J. Bridge Eng.*, 10.1061/(ASCE)1084-0702(2007)12:5(600), 600-610.

Priestley, M. N., Sritharan, S., Conley, J. R., and Pampanin, S. (1999). "Preliminary results and conclusions from the presss five-story precast concrete test building." *PCI J.*, 44(6), 42-67.

Priestley, M. N., and Tao, J. R. (1993). "Seismic response of precast prestressed concrete frames with partially debonded tendons." *PCI J.*, 38(1), 58-69.

Rahman, A. M., and Restrepo, J. I. (2000). "Earthquake resistant precast concrete buildings: Seismic performance of cantilever walls prestressed using unbonded tendons." University of Canterbury, Christchurch, New Zeland

Restrepo, J. I., and Rahman, A. (2007). "Seismic performance of self-centering structural walls incorporating energy dissipators." *J. Struct. Eng.*, 10.1061/(ASCE)0733-9445(2007)133:11(1560), 1560-1570.

Schwer, L. "The winfrith concrete model: Beauty or beast? Insights into the winfrith concrete model." *Proc., 8th European LS-DYNA Users Conf.*, 23-24.

Sritharan, S., Aaleti, S., Henry, R. S., Liu, K.-Y., and Tsai, K.-C. (2015). "Precast concrete wall with end columns (prewec) for earthquake resistant design." *Earthq. Eng. Struct. D.*, 44(12), 2075-2092.

Stanton, J., C. Stone, W., and Cheok, G. (1997). "A hybrid reinforced precast frame for seismic regions." *PCI J.*, 42, 20-23.

Taghdi, M., Bruneau, M., and Saatcioglu, M. (2000). "Seismic retrofitting of low-rise masonry and concrete walls using steel strips." *J. Struct. Eng.*, 10.1061/(ASCE)0733-9445(2000)126:9(1017), 1017-1025.

Viti, S., Cimellaro, G. P., and Reinhorn, A. M. (2006). "Retrofit of a hospital through strength reduction and enhanced damping." *Smart Struct. Syst.*, 2(4), 339-355.

Wallace, J. W. (2012). "Behavior, design, and modeling of structural walls and coupling beams—lessons from recent laboratory tests and earthquakes." *Int. J. Concr. Struct. M.*, 6(1), 3-18.

Yang, C., and Okumus, P. (2017). "Ultrahigh-performance concrete for posttensioned precast bridge piers for seismic resilience." *J. Struct. Eng.*, 10.1061/(ASCE)ST.1943-541X.0001906, 04017161.